Influence of Temperature and Illumination on the Electrical Characteristics of Nanocrystalline Cu_2S Based Heterojunctions for Photodetector Application

H.S. Soliman[a], A.A.M. Farag[a,b,*], M.M. Saadeldin[c] and K. Sawaby[c]

[a]Thin Film Laboratory, Physics Department, Faculty of Education, Ain-Shams University, Cairo 11757, Egypt

[b]Physics Department, Faculty of Science and Arts, Al Jouf University, Al Jouf, Saudi Arabia

[c]Physics Department, Faculty of Science, Cairo University, Giza 12613, Egypt

(Received November 14, 2014)

In this work, heterojunctions of Cu_2S/p-Si were prepared by high vacuum thermal evaporation technique and examined as a photodetector structure. The dark current–voltage (I–V) characteristics of the heterojunctions measured at different temperatures ranging from 303 to 373 K were investigated. The predominant conduction mechanisms, series resistance, ideality factor and potential barrier height were determined. The downward curvature at sufficiently large voltages in the I–V characteristics is caused by the effect of series resistance R_s. The ideality factor obtained from I–V characteristics is larger than unity which can be attributed to the presence of a thin interfacial insulator layer between the metal and semiconductor. The photocurrent properties of the device under reverse bias using various illuminations were also explored for checking the validity of photodetector application of the studied device. The responsivity of light for the device under reverse bias confirms that the Cu_2S/p-Si heterojunctions are valid for photodetector application. Moreover, these results suggest that the fabricated diode can be used for optical sensor applications. The capacitance–voltage characteristics of diode were also investigated at high frequency of 1 MHz.

DOI: 10.12693/APhysPolA.127.1688

PACS: 73.40.Ei, 73.50.Pz

1. Introduction

Binary semiconductors of II–VI have been receiving significant attention for photovoltaic devices. Among these is chalcopyrite-type material, Cu_2S, that possesses some exceptional characteristics for heterojunction application with Si [1, 2].

Copper sulphide (Cu_xS) thin films have received particular attention since Reynolds et al. [3] discussed the CdS/Cu_xS heterojunction solar cell in 1954.

The Cu_xS thin films are effectively used in solid junction solar cells which have many applications as it is a direct energy conversion device [4].

Sartale and Lokhande [4] reported the simple successive ionic layer adsorption and reaction (SILAR) method for production of Cu_xS thin films using copper sulphate and thiourea solutions as cationic and anionic precursors, respectively. They found that the films were amorphous or consisting of fine grains on glass substrate, whereas many-fold increase in crystallinity was observed for Si (1 1 1) wafer substrate.

Yahiya et al. [1] reported a study of the electrical and photoelectric properties of p-Cu_2S/n-Si devices by using chemical spray pyrolysis technique. They investigated the forward current of this junction using the tunneling-recombination model.

In the present work, Cu_2S/p-Si heterojunction was fabricated by deposition of Cu_2S thin films using the thermal evaporation method onto p-Si single crystal. The dependence of the I–V characteristics on the temperature in both forward and reverse bias was studied in an attempt to obtain information on the transport mechanisms of the devices. Moreover, the effect of illumination of the devices under reverse bias to study the responsivity of the device are also explored for checking the validity of photodetector application of the studied device. In addition, capacitance–voltage (C–V) measurements were applied for characterization of these heterojunction. Moreover, photodiode properties have been investigated by illuminated I–V characteristics.

2. Experimental

The Cu_2S powder used in this study was obtained from Sigma Aldrich Company with purity of 99.99% trace metals basis. The p-Si single-crystal substrate was obtained from Nippon Mining Company. Chemical etching of p-Si was performed with $HF:HNO_3:CH_3COOH$ in ratio 1:6:1 for 10 s then rinsed with ethanol and dried. The p-Si substrate was coated from one side by Cu_2S thin film of 200 nm thick using the evaporation technique. Then the Cu_2S layer was over-coated by an Au mesh to be used as ohmic electrode, while an ohmic Al electrode coated the other side of p-Si. The I–V characteristics of the fabricated heterojunction were achieved by measuring the resulted current corresponding to a certain potential difference dropped across the junction, using a conventional circuit for I–V measurement. The voltage across the configuration system and current passing through it, were measured simultaneously using a high impedance electrometers (Keithley 617, 616, respec-

*corresponding author; e-mail: alaafaragg@gmail.com

tively). The dark I–V characteristics were obtained in a complete dark chamber at room temperature or inside a dark furnace in case of measurements at higher temperatures. The dark C–V characteristics for the Cu_2S/p-Si heterojunction were measured at room temperature at 1 MHz, using a computerized 410 C–V meter (Solid State Measurement Inc., Pittsburgh). The temperature was measured directly by mean of hand held Pt–PtRh thermocouple. The cells were exposed to light coming from a light source (white light) to get an intensity of incident power variable by changing the distance between the cell and the light source. The spectral photosensitivity $R_{ph}(A/W)$ is defined as $R_{ph} = I_{ph}/P_{opt}$, where I_{ph} is the photocurrent and P_{opt} is the incident optical power. An Xe arc lamp was used as light source for the wavelength range from 400 to 950 nm using a monochromator.

3. Results and discussions

3.1. Surface morphology characteristics

The surface morphology of the Cu_2S film was studied by scanning electron microscopy (SEM) and shown in Fig. 1. This figure shows a dense, rough coating with irregularly arranged particles that are about 0.5–1 μm in diameter, which can be attributed to the crystal growth and densification. However, fine Cu_2S particles on the top layer of the film are about 10 nm in diameter and they are inhomogeneously distributed over the substrate which are discrete and have a high volume fraction of interspaces. Moreover, the surface has a strong agglomeration tendency, and a relatively rough surface is present.

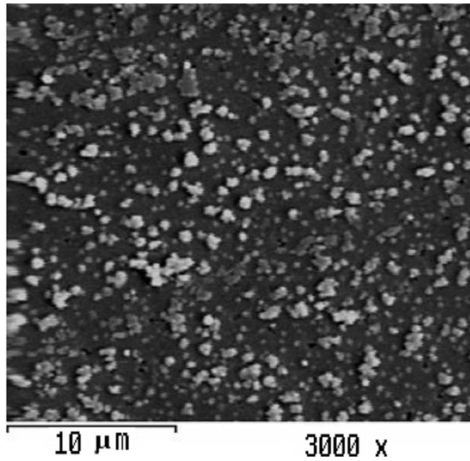

Fig. 1. SEM image of Cu_2S film.

Figure 2a shows a 2D AFM image of Cu_2S film. The surface feature indicates a high agglomeration of fine particles. Figure 2b shows a 3D image where the surface structure indicates that the film is not smooth and the average calculated surface roughness is approximately 3–5 nm.

3.2. Dark current–voltage characteristics

The current–voltage measurements provide a valuable source of information about the junction properties such

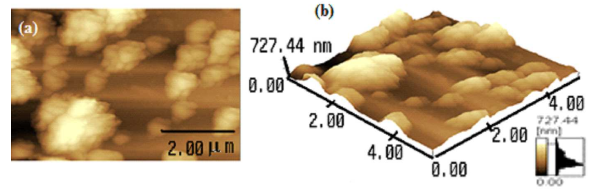

Fig. 2. AFM images of Cu_2S film: (a) 2D image and (b) 3D image.

as the diode quality factor (n), the reverse saturation current (I), the barrier height (Φ_b) and the series resistance (R_s) resistance. Moreover, the analysis of the I–V characteristics is also extremely useful to identify the transport mechanisms controlling the conduction. The $\ln(I$–$V)$ characteristics of Cu_2S/p-Si heterojunction under forward bias were measured in the temperature range 303–423 K and illustrated in Fig. 3. It shows an exponential increase in the forward current with applied voltage for the junction within the narrow low forward voltage ($0 < V_f < 0.3$ V). This exponential dependence at lower voltage range can be attributed to the formation of depletion region between Cu_2S and Si substrate. This behavior can be understood by the formation of a barrier at the interface that limits the flowing of the forward and reverse carriers across the junction, where the potential barrier could be developed [5].

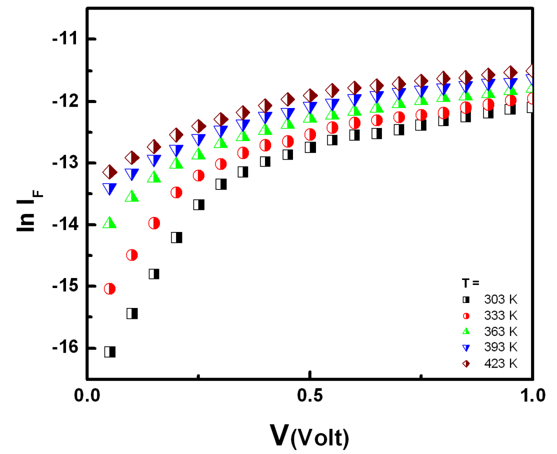

Fig. 3. Plot of $\ln(I_{ph}$–$V)$ characteristics of Cu_2S/p-Si heterojunction at different temperatures.

Thus, the voltage dependence of the junction current can be expressed according to the theory of thermionic emission mechanism and given by [5, 6]:

$$I = I_0 \exp\left(\frac{qV - IR_s}{nkT}\right), \tag{1}$$

where n is the diode ideality factor, k is the Boltzmann constant, q is the charge carrier, R_s is the series resistance, I is the saturation current obtained by extrapolation of the linear $\ln(I$–$V)$ portion to the $\ln I$ axis at zero voltage and can be expressed by the following:

$$I_0 = AA^*T^2 \exp\left(\frac{q\Phi_b}{kT}\right), \quad (2)$$

where Φ_b is the barrier height, A is the diode area and A^* is the effective Richardson constant. Obtaining a straight line from the plot of the semilogarithm of I_0/T^2 against $1/T$, shown in Fig. 4, supports that the predominant current mechanism is due to the thermionic emission mechanism of carriers over the potential barrier of the device [6]. From the slope of this straight line the potential barrier height, Φ_b is determined and found to be $\approx$0.54 eV.

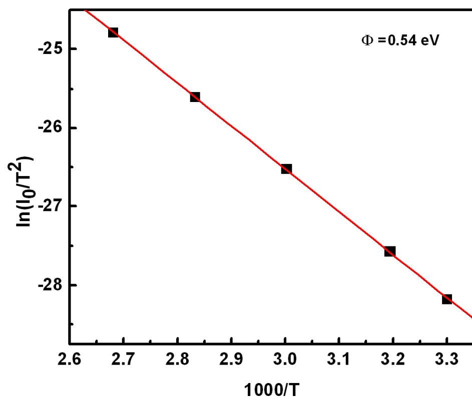

Fig. 4. Plot of $\ln(I_0/T^2)$ vs. $1000/T$ of of Cu_2S/p-Si heterojunction.

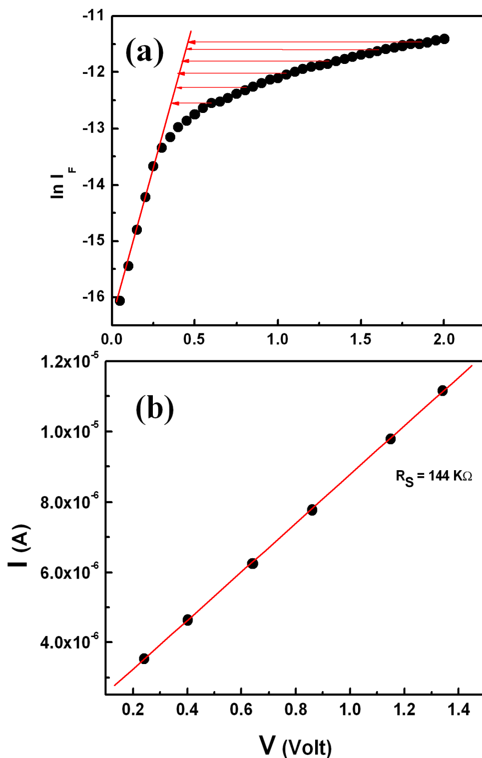

Fig. 5. (a) Plot of $\ln(I_{ph}–V)$ characteristics showing the deviation from linearity for determination R_s; (b) plot of $I–V$ characteristics in the curvature region for determination R_s.

The series resistance R_s of the neutral region of the semiconductor also plays an important role in current–voltage and capacitance–voltage characteristics of the heterojunction, and it causes that the interface state density and their relaxation time obtained from admittance spectroscopy become different from those that would be expected [7, 8]. Due to the existence of the R_s, significant voltage drop is observed at large forward currents. In this case, the semilogarithmic $I–V$ plot deviates from a straight line at high forward bias as shown in Fig. 5. However, the current curve in forward bias becomes quickly dominated by series resistance from contact wires or bulk resistance of the semiconductor, which causes a curvature at high current in the semilogarithmic $I–V$ plot.

Figure 5a could be used to determine R_s of the junction [9]. Thus, for a given I, the horizontal displacement between the actual curve and the extrapolated linear part gives the voltage drop, ΔV ($= IR_s$, across the neutral region). The plot of ΔV vs. I shown in Fig. 5b should give a straight line whose slope yields the value R_s of 144 kΩ. It is clearly obvious that the high value of the obtained series resistance gives evidence for that the R_s value should be taken into account the role of R_s in determining the interface state density distribution profiles of the junction [10]. Similar results have been reported in the literature [11, 12].

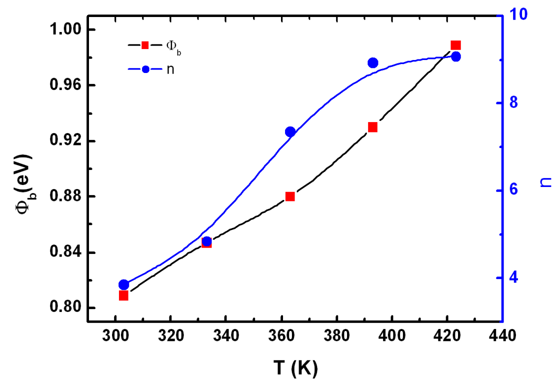

Fig. 6. Plot of Φ_b and n vs. T of Cu_2S/p-Si heterojunction.

The experimental values of the barrier height, Φ_b and the ideality factor, n for the heterojunction were determined from intercepts and slopes of the forward bias $\ln(I–V)$ plot at each temperature. The values of n and Φ_b were obtained from Eqs. (1) and (2), and are presented in Fig. 6, respectively. The ideality factor n is introduced to calculate the deviation of the experimental $I–V$ data from the ideal thermionic model. The value of ideality factor approaches unity for an ideal junction [13]. Deviation of n from unity may be attributed to either recombination of electrons and holes in the depletion region, and/or the increase of the diffusion current due to increasing the applied voltage [14]. As observed from Fig. 6 both parameters are found to be dependent strongly on temperature. This feature can be connected either with the lateral inhomogeneity of barrier height or with the

domination of the current with thermionic field emission [15]. As observed from Fig. 6 the experimental values of Φ_b and n for the heterojunction are changed from 0.81 eV and 3.86 at 303 K to 0.99 eV and 9.1 at 423 K, respectively. The values of Φ_b calculated from forward bias I–V characteristics shows an unusual behavior that increases with the increase of temperature. Such temperature dependence is an obvious disagreement with the reported negative temperature coefficient of the barrier height obtained from reverse bias capacitance–voltage measurements [13]. Also, the value of n is not constant with temperature and increased with increasing temperature. Such behavior of an ideality factor has been attributed to particular distribution of interface states and insulator layer between metal and semiconductor [16–18]. Moreover, the effective barrier height Φ_e, instead of Φ_b, is assumed to be bias-dependent due to the presence of an interfacial insulator layer and interface states located at the heterojunction interface.

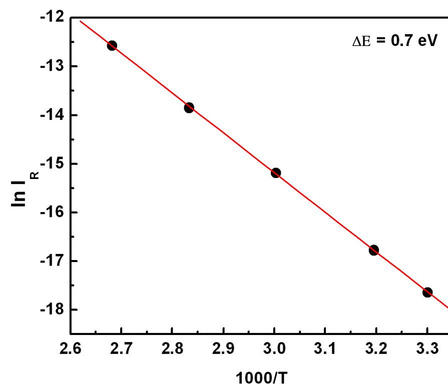

Fig. 7. Plot of $\ln(I_R)$ vs. $1000/T$ of Cu_2S/p-Si heterojunction.

On the other hand, the reverse current–voltage characteristics of Cu_2S/p-Si heterojunction diode at different temperature range were also considered. From these data one can observe a small dependence on voltage assuming that the generation-recombination current is the dominant source of the reverse current of the base heterojunction under consideration and the generation-recombination process occurring via mid band gap states of the p-Si substrate. In case that the main source of the reverse current is generation through Si rather than through the interface or the thin film itself, the reverse current (I_R) can be expressed as follows [19]:

$$I_R = I_0 \exp\left(\frac{-E_g}{2kT}\right), \tag{3}$$

where E_g is the energy gap of the base material. Using the slope of Fig. 7, the obtained activation energy is approximately equal to half the band gap of Si. This suggests that the main source of the reverse current is the Si substrate and can be suggest that the reverse current should be limited by the carrier generation-recombination process occur via mid band gap states.

3.3. Current–voltage Cu_2S/p-Si characteristics under illumination

Current–voltage (I–V) characteristics of Cu_2S/p-Si device under dark and light illumination condition of 80 mW/cm^2 are shown in Fig. 8. The increase in the photocurrent is due to the drift velocity of photogenerated electrons and holes in Si. The photocurrent in the reverse direction is strongly increased by photo-illumination. The current in reverse direction is strongly increased by illumination. This suggests that the Cu_2S/p-Si diode is a photodetector. This behavior yields useful information on the electron–hole pairs which was effectively generated in the junction by incident photons. The photocurrent is higher than the dark current at the same reverse bias. This suggests that the light generates carrier contributing photocurrent due to the production of electron–hole pairs as a result of the light absorption [20].

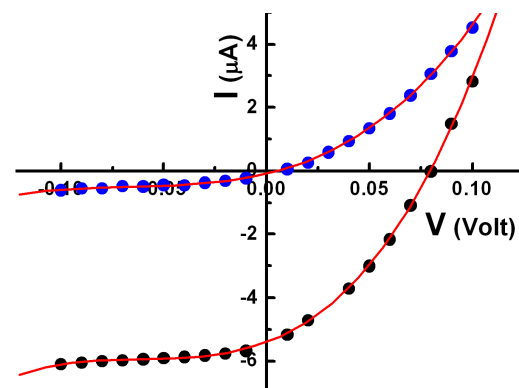

Fig. 8. Plot of dark and illuminated I–V characteristics of Cu_2S/p-Si heterojunction.

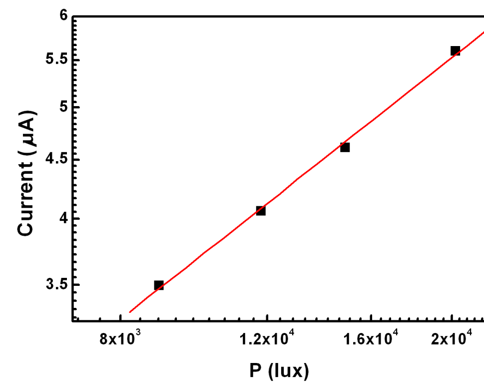

Fig. 9. Plot of photocurrent under different illumination intensity of Cu_2S/p-Si heterojunction.

In order to analyze photoconductivity mechanism of the diode, the variation of the photocurrent with illumination intensity is shown in Fig. 9. The photocurrent increases with increasing illumination intensity which indicates that the light illumination increases production of electron–hole pairs. The photocurrent dependence of light intensity is expressed as [21, 22]:

$$I_{\rm ph} = \chi P^m, \quad (4)$$

where $I_{\rm ph}$ is the photocurrent, χ is a constant, m is an exponent and P is the intensity of the incident light. The value of m was determined from the slope of $\log(I_{\rm ph})$ vs. $\log(P)$ plot and was found to be 0.57. When the value of m is 0.5, this means that the mechanism corresponds to bimolecular recombination. But when the value of m is 1.0, this corresponds to monomolecular recombination mechanism [21, 22]. Whereas the obtained value of the exponent is approximately 0.5, therefore the predominant conduction mechanism is bimolecular recombination.

One can obtain more information by acquiring the detector's spectral response. Figure 10 shows the photocurrent as a function of the wavelength, where the incident light was monochromized by the monochromator and the photocurrent was measured using a 617 electrometer. The particular feature of the photodetector detector is the presence of surface band bending, which allows this device to work without any applied voltage [23]. Illumination of the photodetector structure at a wavelength range of 400–800 nm under reverse bias of −1 V led to the spectral response curves shown in Fig. 10. The high broad peak maximum at around 492 nm may be due to the absorbance band of nano Cu_2S. The present Cu_2S/p-Si shows acceptable sensitivity for the detection of light.

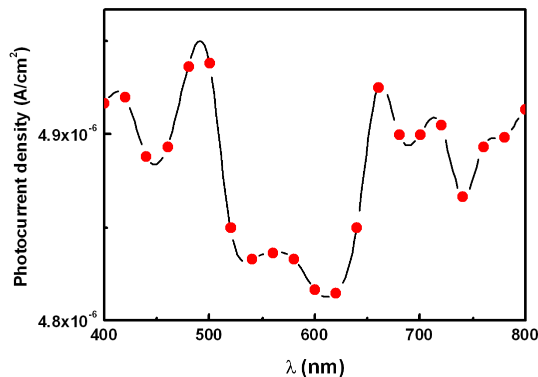

Fig. 10. Plot of photocurrent density vs. wavelength of Cu_2S/p-Si heterojunction.

The dark capacitance–voltage ($1/C^2$–V) characteristics of Cu_2S/p-Si heterojunctions were measured at 1 MHz and shown in Fig. 11. This frequency is high enough to neglect the dielectric relaxation process in Cu_2S film [24] and get information on the depletion region extended in the p-Si side. The C–V characteristics of Cu_2S/p-Si heterojunctions can be expressed as follows:

$$\frac{1}{C^2} = \frac{2\,(V_{\rm b} - V)}{qA^2\varepsilon\varepsilon_0 N_A}, \quad (5)$$

where A is the area of the diode, $V_{\rm b}$ is the diffusion voltage (built-in potential) at zero bias which is determined from the intercept of $1/C^2$–V plot, N_A is the ionized traps like-acceptor determined from the slope of $1/C^2$–V plot, ε is the dielectric constant of the semiconductor

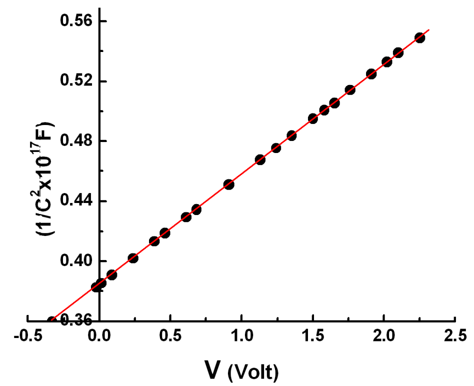

Fig. 11. Plot of $1/C^2$–V characteristics of Cu_2S/p-Si heterojunction.

(≈11.8 for Si) and ε is the dielectric constant of vacuum (≈8.85×10^{-12} F/m). The values of $V_{\rm b}$ and N_A were obtained to be 0.25 eV and 1.75×10^{13} cm^{-3}, respectively.

4. Conclusion

Heterojunctions of Cu_2S/p-Si were fabricated using thermal evaporation technique under vacuum. The ideality factor and barrier height of the diode were found to be 4 and 0.53 eV, respectively. The deviation from the ideal behavior is explained on the basis of series resistance. The photoresponse has been investigated by photocurrent measurements. The I–V characteristics under different light intensity suggest that the photoresponse of the junction is very sensitive to light intensity and the predominant conduction mechanism is bimolecular recombination. The C–V measurements indicate that the capacitance is independent of the voltage and frequency at higher positive voltage. The high value of capacitance at low frequency in reverse bias region is attributed to the excess capacitance resulting from the interface states that could follow the AC signal.

References

[1] C. Song, H. Yin, N. Zhang, S. Li, B. Zhao, K. Yu, *Mater. Lett.* **137**, 56 (2014).

[2] C. Papadopoulos, *Solid State Electronic Devices*, Springer, New York 2014.

[3] D.C. Reynolds, G. Leies, L.T. Antes, R.E. Margurber, *Phys. Rev.* **96**, 533 (1954).

[4] S.D. Sartale, C.D. Lokhande, *Mater. Chem. Phys.* **65**, 63 (2000).

[5] M.M. El-Nahass, K.F. Abd-El-Rahman, A.A.A. Darwish, *Microelectron. J.* **38**, 91 (2007).

[6] M.S. Sze, , K. K. Ng *Physics of Semiconductor Devices*, 3nd ed., Wiley, New York 2007.

[7] S. Karatas, A. Turut, *Vacuum* **74**, 45 (2004).

[8] E. Ayyıldız, C. Nuhoglu, A. Turut, *Electron. Mater.* **31**, 119 (2002).

[9] S. Riad, *Thin Solid Films* **370**, 253 (2000).

[10] A. Tataroglu, S. Altındal, *Microelectron. Eng.* **85**, 233 (2008).

[11] H.A. Cetinkara, A. Turut, D.M. Zengin, S. Erel, *Appl. Surf. Sci.* **207**, 190 (2003).

[12] S. Altındal, S. Karadeniz, N. Tugluoglu, A. Tataroglu, *Solid State Electron.* **47**, 1847 (2003).

[13] A. Tataroglu, S. Altındal, *J. Alloys Comp.* **484**, 405 (2009).

[14] H. Matsuura, *J. Appl. Phys.* **64**, 1964 (1988).

[15] J.P. Sullivan, R.T. Tung, M.R. Pinto, W.R. Graham, *J. Appl. Phys.* **70**, 7403 (1991).

[16] S. Altındal, H. Kanbur, A. Tataroglu, M.M. Bulbul, *Physica B* **399**, 146 (2007).

[17] A. Tataroglu, S. Altındal, *Microelectron. Eng.* **83**, 582 (2006).

[18] I. Dökme, S. Altındal, *Semicond. Sci. Technol.* **21**, 1053 (2006).

[19] M.M. El-Nahass, H.E.A. El-Sayed, A.M.A. El-Barry, *Solid-State Electron.* **50**, 355 (2006).

[20] A. Kavokin, G. Eramo, *Nature Sci.* **2**, 63 (2010).

[21] D.T. Phan, R.K. Gupta, G.S. Chung, A.A. Al-Ghamdi, O.A. Al-Hartomy, F. El-Tantawy, F. Yakuphanoglu, *Sol. Energy* **86**, 2961 (2012).

[22] G.D. Sharma, S.G. Sandogaker, M.S. Roy, *Thin Solid Films* **278**, 129 (1996).

[23] F. Hun, Y. Huang, X. Ren, X. Duan, X. Zhang, X. Fan, W. Wang, Y. Shang, S. Cai, *Opt. Laser Technol.* **48**, 389 (2013).

[24] H.S. Soliman, A.A.M. Farag, N.M. Khosifan, M.M. El-Nahass, *Thin Solid Films* **516**, 8678 (2008).